Proc. of the International Conference on Mechanochemistry and Mechanical Alloying, Kraków, Poland, June 22–26, 2014

Mechanosynthesis and Sintering of $Ce_{1-x}Y_xO_{2-\delta}$ ($x \leq 0.35$) Solid Solutions

M. Fabián*, J. Briančin, T. Schutz
Institute of Geotechnics SAS, Watsonova 45, 04001 Košice, Slovakia

One-step mechanochemical approach was used to synthesize nanocrystalline $Ce_{1-x}Y_xO_{2-\delta}$ ($x \leq 0.35$) solid solutions. X-ray powder diffraction was utilized to characterize crystalline phases of as-prepared products. It was shown that the presence of yttrium suppresses the crystal growth. The effect of yttrium content on the grain size before and after sintering of green bodies at high temperatures was evaluated by means of scanning electron microscopy. The combination of one-step mechanochemical process and relatively low sintering temperatures resulted in preparation of ceria-based ceramics with wide scale of possible applications.

DOI: 10.12693/APhysPolA.126.951
PACS: 61.72.U–, 81.07.Bc, 81.05.Je

1. Introduction

It is well known that CeO_2 (ceria) has been extensively investigated in various applications including catalysts, fuel cells, polishing materials, ultraviolet absorbers, phosphors, oxygen sensors, etc. [1]. It possesses a cubic fluorite structure ($S.C.Fm\bar{3}m$) which is known to tolerate a considerable reduction in size without phase change especially at high temperatures. Moreover, the modification of CeO_2 conductivity properties by means of aliovalent doping has been significantly investigated over last years. In this context, it is generally accepted that doping by Gd^{3+} and Sm^{3+} exhibits the highest conductivity due to the small association enthalpy between dopant cation and oxygen vacancy in the fluorite lattice [2]. However, the high cost prevented their commercial applications. Therefore Y^{3+} doped ceria has been considered as a low-cost material for intermediate-temperature solid oxide fuel cell (SOFC) electrolytes with acceptable electrochemical properties [3].

The synthesis of nanosized doped ceria powders is of immense importance to get dense sintered product at lower temperatures [4]. Many methods have been used to synthesize nanocrystalline CeO_2 doped powders (see e.g. [5, 6] and references therein). Most of them involved complicated steps and expensive raw materials. On the other hand, relatively simple one-step ball milling toward preparation of aliovalent doped CeO_2 presents an alternative method to produce lower-cost powders in the nanometer range [7].

In this work, $Ce_{1-x}Y_xO_{2-\delta}$ ($x = 0$–0.35) solid solutions have been prepared via on step mechanochemical route. The paper evaluates the effect of preparation method and dopant concentration on properties and morphology of sintered specimens.

*corresponding author; e-mail: fabianm@saske.sk

2. Experimental methods

The solid precursors, cerium oxide (CeO_2, 99.9% purity; Aldrich) and yttrium oxide (Y_2O_3, 99.99% purity; Aldrich) were used for the mechanosynthesis of $Ce_{1-x}Y_xO_{2-\delta}$. 5 g of the $(1-x)CeO_2 + (x/2)Y_2O_3$ mixtures ($x = 0.1$–0.35) were milled for various times (up to 90 min) in a high-energy planetary ball mill Pulverisette 7 Premium line (Fritsch). A grinding chamber (80 cm^3 in volume) and balls (10 mm in diameter) made of tungsten carbide were used. The ball-to-powder weight ratio was 40:1. Milling experiments were performed in ambient atmosphere at 600 rpm. For sintering study, as-prepared powders were compacted in a uniaxial hydraulic press at 200 MPa containing 5 wt. % of cellulose. The green pellets were sintered at 1250 °C for 4 h under static air.

The X-ray powder diffraction (XRPD) patterns were collected using a D8 Advance diffractometer (Brucker, Germany) (for phase evolution analysis) and using a X´pert MPD (Phillips, Netherlands) (for sintered samples) both with the Cu $K_{\alpha_{1,2}}$ wavelength in the Bragg–Brentano configuration. The generators were set-up at 40 kV and 40 mA and patterns were collected in the range of 20–85° 2θ with a step of 0.05° 2θ and a time per each step of 5 s. The microstructural analysis of the as-prepared and sintered samples was carried out by field emission scanning electron microscope FE-SEM, Mira 3 (Tescan, Czech Republic) coupled with EDS analyzer (Oxford Instruments, UK). The particle size distribution of as-prepared solid solutions was performed using a PCCS Nanophox (Sympatec, Germany).

3. Results and discussion

The X-ray diffraction patterns of the $Ce_{1-x}Y_xO_{2-\delta}$ ($x = 0$–0.35) solid solutions (where $\delta = x/2$ is the theoretical vacancy concentration) prepared via 90 min of high-energy ball milling are shown in Fig. 1. It can be seen that effective incorporation of yttrium into the fluorite-type structure of ceria results in continuous shift

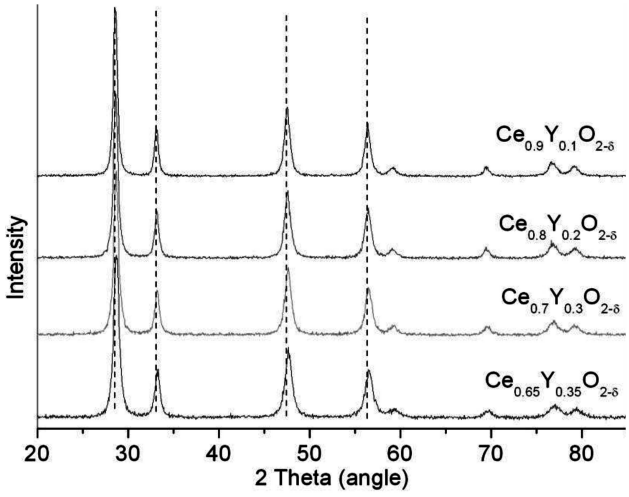

Fig. 1. The XRPD pattern of $Ce_{1-x}Y_xO_{2-\delta}$ ($x = 0-0.35$) solid solutions synthesized via high-energy ball milling.

of all characteristic XRPD reflections to the higher angular positions (lower values of d-spacing), indicating a lattice contraction due to the incorporation of Y^{3+} in the CeO_2 structure. No CeO_2 and Y_2O_3 remaining traces as well as tungsten carbide abrasion was found after ball milling process. The broadening of XRPD peaks reflects the nanocrystalline character (decrease in crystalline size) and increase in lattice strain. This is confirmed by profile analysis of diffraction peaks (see Table) utilizing the Thompson–Cox–Hastings approximation of the Voigt function comprising the size and strain calculations based on integral breadths [8]. Table 1.

TABLE I

The effect of yttrium content on the crystallite and particle size.

Y^{3+} content	Crystallite size/ nm (XRPD)	Particle size/ nm (PCCS)
0.0	21	–
0.1	17	280
0.2	17	300
0.3	14	260
0.35	17	283

Based on the calculation of crystallite size it can be concluded that the presence of yttrium in the ceria samples suppresses their crystallization (crystallite growth); i.e., the average crystallite size of mechanosynthesized $Ce_{1-x}Y_xO_{2-\delta}$ ($x = 0.1-0.35$) ranges from $\approx$ 14 to $\approx$ 17 nm — see Table. This result is in accordance with the findings on Sm^{3+} doped $CeO_{2-\delta}$, see, e.g., Ref. [9] and citations therein as well as with recent work on Eu^{3+} doped $CeO_{2-\delta}$ system [10]. The observed phenomenon can be partly explained by the absence of oxygen (by the presence of oxygen vacancies) in the as-prepared $Ce_{1-x}Y_xO_{2-\delta}$ causing the breaking of bonds between the atomic planes and, thus, resulting in a relatively small grain size, as it has been suggested by Colis et al. [11].

However, relatively big agglomerates resulted from high-energy ball milling with particles size distribution in the range of $\approx$ 250–300 nm. The tendency to form agglomerates as well as homogeneous distribution of particular elements is further confirmed in Fig. 2.

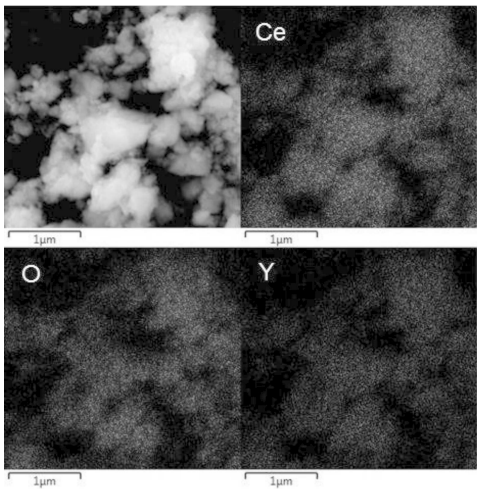

Fig. 2. The particles morphology and elements distribution in mechanosynthesized $Ce_{0.7}Y_{0.3}O_{2-\delta}$.

These results are in the good accordance with PCCS analysis summarized in Table. Moreover, it can be clearly seen that all investigated elements are uniformly distributed over the as-prepared sample confirming the homogeneity of the solid solution.

In order to obtain dense samples, the mechanosynthesized nanopowders were sintered at 1250 °C for 4 h in atmospheric conditions. The $Ce_{1-x}Y_xO_{2-\delta}$ diffraction patterns are essentially unchanged implying that no parasitic phases are present and no phase related transformation had occurred during high-thermal treatment.

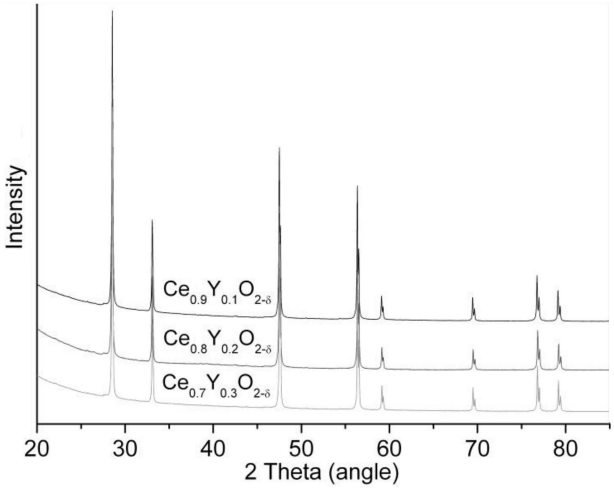

Fig. 3. The XRPD pattern of sintered $Ce_{1-x}Y_xO_{2-\delta}$ ($x = 0.1-0.3$) solid solutions.

As it is shown in Fig. 3, the diffraction peaks became sharp after sintering, indicating high crystallization and increase of the crystallite size. The crystallites size of $Ce_{1-x}Y_xO_{2-\delta}$ ($x = 0.1$–0.35) was found to be in the range of 110–118 nm (110 nm for $x = 0$, 116 nm for $x = 0.1$, 118 nm for $x = 0.2$ and 115 nm for $x = 0.3$, respectively).

Figure 4 shows SEM micrographs of three sintered samples with nominal composition of CeO_2, $Ce_{0.9}O_{0.1}O_{2-\delta}$ and $Ce_{0.7}O_{0.3}O_{2-\delta}$, respectively. It was found that the concentration of small closed pores present in the sample increases with increase of yttrium content.

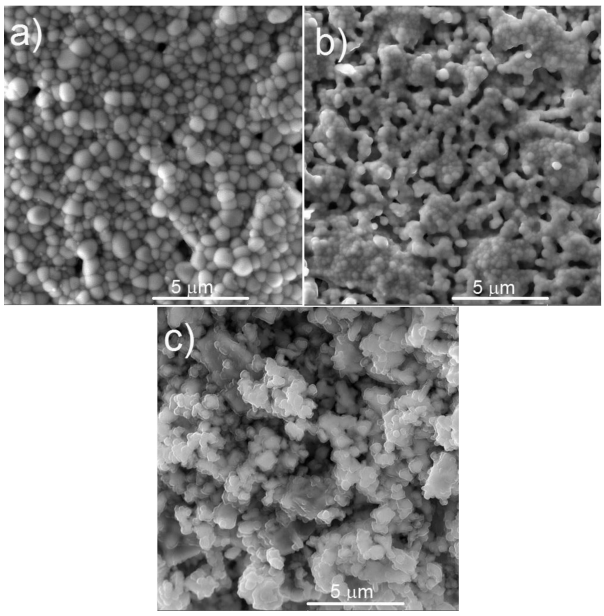

Fig. 4. The SEM micrographs of $Ce_{1-x}Y_xO_{2-\delta}$ pellets sintered for 4 h at 1250 °C. (a) $x = 0$, (b) $x = 0.1$, and (c) $x = 0.3$.

As it was reported [12], the grain size is very important for the crystal structure because at high operating SOFC temperatures high grain sizes result in cracks. The nano-sized fine-grained oxide structure is advantageous. This is so because the diffusion can easily take place and release the accumulated stresses at high temperatures for large grain sized crystalline ceramic structures [13]. On the other hand, it was found that the highest values of electronic conduction are reached with dopant concentration up to 10 mol.% [14]. It also implies that the conductivity is influenced by presence of small pores in the ceria based solid solutions.

4. Conclusions

The one-step mechanosynthesis has been successfully employed to prepare $Ce_{1-x}Y_xO_{2-\delta}$ ($x = 0.1$–0.35) solid solutions with a crystallite average size below 20 nm. Yttrium incorporation into the F-type ceria structure was confirmed by XRPD. The effect of yttrium concentration on structural and microstructural parameters of sintered samples was investigated by FE-SEM. It was found that increase in yttrium content results in formation of small pores distributed in solid solution.

Acknowledgments

The financial support by the Slovak Research Grant Agency (project VEGA 2/0097/13) and Slovak Research and Development Agency (APVV-0189-10) is gratefully acknowledged.

References

[1] X. Song, N. Jiang, Y. Li, D. Xu, G. Qiu, *J. Rare Earth* **25**, 428 (2007).

[2] G. Laukaitis, J. Dudonis, *J. Alloy. Comp.* **459**, 320 (2008).

[3] B. Zhu, X. Liu, P. Zhou, Z. Zhu, W. Zhu, S. Zhou, *J. Mater. Sci. Lett.* **20**, 591 (2001).

[4] H. Xu, H. Yan, Z. Chen, *J. Power Sources* **163**, 409 (2006).

[5] A. Arabaci, M.F. Öksüzömer, *Ceram. Int.* **38**, 6509 (2012).

[6] C. Goulart, E. Djurado, *J. Eur. Ceram. Soc.* **33**, 769 (2013).

[7] P. Baláž, M. Achimovičová, M. Baláž, P. Billik, Z. Cherkezova-Zheleva, J.M. Criado, F. Delogu, E. Dutkova, E. Gaffet, F.J. Gotor, R. Kumar, I. Mitov, T. Rojac, M. Senna, A. Streletskii, K. Wieczorek-Ciurowa, *Chem. Soc. Rev.* **42**, 7571 (2013).

[8] J. Rodriguez-Carvajal, *Physica B* **192**, 55 (1993).

[9] L. Živković, V. Lair, O. Lupan, A. Ringuedé, *Thin Solid Films* **519**, 3538 (2011).

[10] A. Kremenović, D.K. Bozanić, A.M. Welsch, B. Jancar, A.S. Nikolić, M. Bošković, Ph. Colomban, M. Fabian, B. Antić, *J.Nanosci. Nanotechnol.* **12**, 8893 (2012).

[11] S. Colis, A. Bouaine, G. Schmerber, C. Uhlaq-Bouillet, A. Dinia, S. Choua, P. Turek, *Phys. Chem. Chem. Phys.* **14**, 7256 (2012).

[12] I. Uslu, A. Aytimur, M.K. Öztürk, S. Koçyiğit, *Ceram. Int.* **38**, 4943 (2012).

[13] Z.Y. Liu, W. Gao, K. Dahm, F.H. Wang, *Scr. Mater.* **37**, 1551 (1997).